Robust Adaptive Fixed-Time Sliding-Mode Control for Uncertain Robotic Systems With Input Saturation

Yunsong Hu, Huaicheng Yan, Hao Zhang, Meng Wang, and Lu Zeng

***Abstract*—In this article, a robust adaptive fixed-time sliding-mode control method is proposed for robotic systems with parameter uncertainties and input saturation. First, a model-based fixed-time controller is designed under the premise that the system parameters are known. Moreover, the unknown dynamics of robotic systems and the boundary of compounded disturbance are synthesized into a compounded uncertainty. Then, the Gaussian radial basis function neural networks (NNs) are selected to approximate the compounded uncertainty. In addition, the nonsingular fast terminal sliding-mode (NFTSM) control is incorporated into the proposed fixed-time control framework to enhance the robustness and convergence speed of unknown robotic systems. Finally, a comparative simulation based on a rigid manipulator shows the superiority and efficacy of the designed methods.**

***Index Terms*—Fixed-time control, input saturation, neural networks (NNs), nonsingular fast terminal sliding mode (NFTSM).**

I. Introduction

NOWADAYS, robotic technology has made a qualitative leap forward. However, robots belong to a class of high coupled nonlinear multi-input–multi-output (MIMO) systems, whose performance can easily deteriorate when they encounter uncertainties and external disturbances. For this reason, how to overcome such limitations and further improve the control performance is a valuable research hotspot.

In order to cope with the aforementioned problem, numerous methods have been proposed in the existing research, such as adaptive control [1], [2]; active disturbance rejection control (ADRC) [3]; model predictive control [4], [5]; robust control [6]; backstepping control [7], [8]; fuzzy control [9]–[14]; sliding-mode control [15]–[18]; neural-networks (NNs) control [19]–[23]; etc. Compared with other methods, sliding-mode control has an outstanding property of insensitivity to external disturbances. Linear sliding-mode (LSM) control can ensure the state variables converge to zero asymptotically. However, the convergence time cannot be guaranteed. To address this problem, terminal sliding-mode (TSM) control is designed to enhance the convergence properties of the dynamical systems and achieve the finite-time convergence. Inspired by this, for ensuring that the robotic manipulator with parameter uncertainties and external disturbances tracks the trajectory with high precision in finite time, the authors proposed a chattering-free integral TSM control scheme in [24]. Compared with TSM control, a novel control method called fast TSM (FTSM) control has a more satisfactory performance in terms of convergence speed. However, the aforementioned methods may encounter the singularity problem. In order to eliminate the singular problem, nonsingular TSM (NTSM) control [25] and nonsingular FTSM (NFTSM) control [26] have been proposed. Compared with the NTSM control, the NFTSM control provides a faster state convergence.

Noteworthily, a great deal of literature on robots mainly concentrated on the finite-time control. It is recognized that the major weakness of finite-time control for robots is the convergence time of tracking errors that depends on the initial conditions of the designed system. Fortunately, fixed-time control has been designed to overcome this weakness. Compared with finite-time control, the fixed-time control guarantees that state variables of the system have a uniformly bounded convergence time, and this upper boundary is independent of the initial conditions [27], [28]. Therefore, the fixed-time control strategy has received plentiful research attention in recent decades. A NFTSM control method was proposed to deal with the consensus tracking problem of the multiagent system [29].

Manuscript received 10 June 2021; revised 9 November 2021 and 28 February 2022; accepted 25 March 2022. Date of publication 20 April 2022; date of current version 16 March 2023. This work was supported in part by the National Natural Science Foundation of China under Grant 62173146, Grant 62073143, Grant 61922063, and Grant 62003139; in part by the Shanghai Natural Science Foundation under Grant 22ZR1416200 and Grant 20ZR1415200; in part by the Program of Shanghai Academic Research Leader under Grant 19XD1421000; in part by the Shanghai and HongKong–Macao–Taiwan Science and Technology Cooperation Project under Grant 19510760200; in part by the Shanghai Shuguang Project under Grant 18SG18; and in part by the Innovation Program of Shanghai Municipal Education Commission under Grant 2021-01-07-00-02-E00107. This article was recommended by Associate Editor H. Zhang. *(Corresponding author: Huaicheng Yan.)*

Yunsong Hu and Meng Wang are with the Key Laboratory of Smart Manufacturing in Energy Chemical Process of Ministry of Education, East China University of Science and Technology, Shanghai 200237, China.

Huaicheng Yan is with the Key Laboratory of Smart Manufacturing in Energy Chemical Process of Ministry of Education, East China University of Science and Technology, Shanghai 200237, China, and also with the School of Information Science and Engineering, Chengdu University, Chengdu 610106, China (e-mail: hcyan@ecust.edu.cn).

Hao Zhang is with the Department of Control Science and Engineering, Tongji University, Shanghai 200092, China (e-mail: zhang_hao@tongji.edu.cn).

Lu Zeng is with the Academy for Engineering and Technology, Fudan University, Shanghai 200433, China (e-mail: 20110860044@fudan.edu.cn).

Color versions of one or more figures in this article are available at https://doi.org/10.1109/TCYB.2022.3164739.

Digital Object Identifier 10.1109/TCYB.2022.3164739

2168-2267 © 2022 IEEE. Personal use is permitted, but republication/redistribution requires IEEE permission.
See https://www.ieee.org/publications/rights/index.html for more information.

Authorized licensed use limited to: CHONGQING UNIVERSITY. Downloaded on May 15,2023 at 10:16:35 UTC from IEEE Xplore. Restrictions apply.

Shi *et al.* [30] extended the standard sliding-mode system and proposed a novel fixed-time high-order sliding-mode (HOSM) control scheme. In order to avoid the singularity problem, a piecewise sliding-mode surface was proposed in [31] to ensure that the system state was practical fixed-time stable. Yang [32] guaranteed the convergence of the tracking errors at a specified time by selecting parameters that satisfy certain constraints.

One obvious limitation of the above methods is that the specific parameters of the dynamic system need to be known in advance, but it is difficult to be guaranteed in practical applications. NNs control is extensively used to deal with uncertainties and nonlinearities in system models. Besides, the input saturation issue in the robotic systems also needs to be paid attention too. Zhang *et al.* [33] designed a fault-tolerant controller which combined sliding-mode control with NNs control. A NNs-based fixed-time controller was proposed to tackle the situation of the input dead zone of the robot in [35]. In [36], a piecewise function was established to describe input constraints. In the process of the controller design, the controller was also designed to offset the impact of input constraints by the segmented design. Zhu and Du [37] designed an auxiliary dynamic system to eliminate the influence of input saturation. However, these methods can increase the complexity of the controller and are difficult to generalize to other systems.

It is worth noting that the considered aspects in the aforementioned papers include fixed-time control, sliding-mode control, NNs, and input saturation. However, few results consider the above issues uniformly in uncertain robotic systems. Based on the aforementioned observations, this article focuses on the design of robust adaptive fixed-time sliding-mode control for uncertain robotic systems with input saturation. The main contributions of this article can be described as summarized as follows.

1) Different from the finite-time control methods proposed in literature [24]–[26], the fixed-time control scheme is designed in this article, which can ensure that the convergence time of the system states is uniformly bounded, and the upper bound of the convergence time only depends on the preset parameters. Furthermore, parameter selection in this article does not need to satisfy the complex constraints in [32], which contributes to more design flexibility.
2) By using the arctangent function to approximate the saturation function and combining with the mean value theorem, the proposed controller can effectively deal with the adverse impact caused by input saturation. Compared with the existing methods [35]–[37], our method has a more concise structure and is suitable to be extended to other systems.
3) In the process of the controller design, sliding-mode control, fixed-time control, and NNs are integrated to solve the tracking control problem of unknown robotic systems with input saturation. Previous works only investigate one or some of these aspects. Therefore, accurate system parameters are no longer known in advance, and the robustness of the system is improved, which helps to improve the freedom of designing controllers and achieve better performance.

This article is described in the following sections. Section II formulates the mathematical model of the rigid robotic manipulator and several lemmas are used in this article. The design process of the controller and stability analysis are expressed in Section III. In Section IV, the simulations are conducted to illustrate the validity and feasibility of the proposed method. Finally, Section V draws the conclusion of this article.

II. Problem Formulation and Preliminaries

A. System Model

The dynamics model of a rigid manipulator can be expressed as the following formulation:

$$M(q)\ddot{q} + C(q,\dot{q})\dot{q} + g(q) = \tau + d(t) \tag{1}$$

where $q, \dot{q}, \ddot{q} \in \mathbb{R}^n$ denote the position, velocity, and acceleration, respectively, $M(q) \in \mathbb{R}^{n\times n}$ is the symmetric and positive-definite inertia matrix, $C(q,\dot{q}) \in \mathbb{R}^{n\times n}$ represents the centripetal–coriolis matrix, $g(q) \in \mathbb{R}^n$ stands for the vector of gravity, $d(t) \in \mathbb{R}^n$ represents the external disturbance vector, and $\tau \in \mathbb{R}^n$ is the torque input vector. Then, M, C, g, and d will be used to simplify the expression in the subsequent design process.

Assumption 1: The external disturbance $d_i(t)$ is unknown bounded and satisfies $|d_i(t)| \le \bar{d}_i (i = 1, 2, \ldots, n)$, where $\bar{d}_i$ is a positive constant.

Assumption 2: The desired trajectory $q_d(t)$ and its derivatives ${q_d}^{(i)}(t) (i = 1, 2)$ are known and bounded.

Remark 1: The external disturbance of the robotic system is mainly composed of friction force, which is always bounded in practical systems. Therefore, it is reasonable to suppose the external disturbance term $|d_i(t)|$ is bounded. Such assumption can be found in [33]. Assumption 2 is very common, and such assumption can be seen in [38].

B. Input Saturation

In practice, the actuator inevitably suffers from the input saturation. Therefore, the designed control input $u(t) \in \mathbb{R}^n$ is subject to saturation nonlinearity and can be formulated as follows:

$$\tau(u(t)) = \begin{cases} \mathrm{sign}(u(t))\tau_M, & |u(t)| \ge \tau_M \\ u(t), & |u(t)| < \tau_M \end{cases} \tag{2}$$

where τ_M denotes the maximum amplitude of the control input. To efficiently tackle the saturation problem, the actuator saturation can be approximated by [39]

$$\begin{aligned} \tau_i(u_i) &= g_i(u_i) + \Delta\tau_i(u_i) \\ &= \frac{2\tau_{iM}}{\pi}\arctan\left(\frac{\pi u_i}{2\tau_{iM}}\right) + \Delta\tau_i(u_i) \end{aligned} \tag{3}$$

where $\Delta\tau_i(u_i)$ with $i = 1, 2, \ldots, n$ represents the bounded approximation error, and then we have

$$|\Delta\tau_i(u_i)| \le \tau_{iM} - \frac{2\tau_{iM}}{\pi}\arctan\left(\frac{\pi}{2}\right) = \bar{\Delta}_i. \tag{4}$$

Authorized licensed use limited to: CHONGQING UNIVERSITY. Downloaded on May 15,2023 at 10:16:35 UTC from IEEE Xplore. Restrictions apply.

According to the mean value theorem, $g_i(u_i)$ with $i = 1, 2, \ldots, n$ can be formulated as follows:

$$g_i(u_i) = g_i\left(u_i{}^0\right) + \left.\frac{\partial g_i(u_i)}{\partial u_i}\right|_{u_i = u_i^{\mu_i}} \left(u_i - u_i{}^0\right) \tag{5}$$

where $u_i^{\mu_i} = \mu_i u_i + (1 - \mu_i) u_i^0$ with $0 < \mu_i < 1$.

By choosing $u_i^0 = 0$, we obtain

$$g_i(u_i) = \left.\frac{\partial g_i(u_i)}{\partial u_i}\right|_{u_i = u_i^{\mu_i}} u_i. \tag{6}$$

Define $\Lambda = \mathrm{diag}[(\pi \mu_i u_i / 2\tau_{iM})^2 / (1 + (\pi \mu_i u_i / 2\tau_{iM})^2)] \in \mathbb{R}^{n \times n}$ and $g(u)$ can be reformulated in the following form:

$$g(u) = u - \Lambda u. \tag{7}$$

C. Radial Basis Function Neural Networks

On account of the RBFNNs can approximate any continuous function, they are used to approximate the uncertainty of the system, and then they can be obtained as follows [34]:

$$f_i(X) = W_i{}^T S_i(X), \quad i = 1, 2, \ldots, n \tag{8}$$

where the weight vector $W_i \in \mathbb{R}^l$ with $l > 1$ is the number of hidden layer nodes, the input vector $X = [X_1, X_2, \ldots, X_q]^T$, and the basis function vector $S_i(X) = [s_1, s_2, \ldots, s_l]^T$. According to the universal approximation theorem, it can be concluded that $f_i(X)$ can approximate the function with any desired accuracy when l is chosen large enough. $f_i(X)$ is achieved as follows:

$$f_i(X) = W_i{}^{*T} S_i(X) + \varepsilon_i(X), \quad i = 1, 2, \ldots, n \tag{9}$$

where $\varepsilon_i(X)$ is an approximate error and satisfies $|\varepsilon_i(X)| \le \bar{\varepsilon}_i$ $\forall X \in \Omega_X$ with a positive constant $\bar{\varepsilon}_i$. $W_i{}^*$ is a given ideal constant weight vector and it can be capable of minimizing the approximate error $|\varepsilon_i(X)|$, that is,

$$W_i{}^* = \arg \min_{W_i \in \mathbb{R}^l} \left\{ \sup_{X \in \Omega_X} \left| f_i(X) - W_i{}^T S_i(X) \right| \right\}. \tag{10}$$

Then, $s_j(X)$ is chosen as the Gaussian function, that is

$$s_j(X) = \exp\left[\frac{-\left(X - \mu_j\right)^T \left(X - \mu_j\right)}{\eta_j{}^2} \right], \quad j = 1, 2, \ldots, l \tag{11}$$

where η_j and $\mu_j = [\mu_{j1}, \mu_{j2}, \ldots, \mu_{jq}]^T$ are the width of the Gaussian function and the center of receptive field, respectively.

D. Preliminaries

Definition 1 [27]: Consider the following nonlinear system:

$$\dot{x} = g(t, x), \quad x(0) = x_0 \tag{12}$$

where $x \in \mathbb{R}^n$ and $g : \mathbb{R}^+ \times \mathbb{R}^n \to \mathbb{R}^n$. The equilibrium point of the system satisfies the definition of fixed-time stable if it is globally finite-time stable and the settling time function $T(x_0)$ is uniformly bounded, that is, $T(x_0) \le T_{\max}$, $T_{\max} > 0$ $\forall x_0 \in \mathbb{R}^n$.

Lemma 1 [40]: Assuming there exists a Lyapunov function $V(x)$, the following formulation is valid:

$$\dot{V}(x) < -\varphi V^a(x) - \theta V^b(x) \tag{13}$$

where $\varphi > 0$, $\theta > 0$, $a > 1$, and $0 < b < 1$. Then, we can conclude that the equilibrium point of the system is fixed-time stable, and the settling time T satisfies the following inequality:

$$T \le T_{\max} = \frac{1}{\varphi(a - 1)} + \frac{1}{\theta(1 - b)}. \tag{14}$$

Lemma 2 [41]: Assuming that there is a Lyapunov function $V(x)$:$\mathbb{R}^n \to \mathbb{R}$, and then the following inequality is true:

$$\dot{V}(x) < -\varphi V^a(x) - \theta V^b(x) + \zeta \tag{15}$$

where $\varphi > 0, \theta > 0, a > 1, 0 < b < 1$, and ζ being constants. Then, the system is practical fixed-time stable and the fixed time T satisfies the following inequality:

$$T \le T_{\max} = \frac{1}{\varphi v(a - 1)} + \frac{1}{\theta v(1 - b)}. \tag{16}$$

In addition, the residual set of the solution of system (15) can be given by

$$\Omega_x = \left\{ x \mid V(x) \le \min\left\{ \left[\frac{\zeta}{\varphi(1 - v)}\right]^{\frac{1}{a}}, \left[\frac{\zeta}{\theta(1 - v)}\right]^{\frac{1}{b}} \right\} \right\}$$
$$0 < v < 1. \tag{17}$$

Lemma 3 [29]: For any scalars $x_i \in \mathbb{R}$, $i = 1, 2, \ldots, n$, $0 < r_1 < 1$, and $r_2 > 1$, the following inequalities are valid:

$$\left(\sum_{i=1}^{n} |x_i|\right)^{r_1} \le \sum_{i=1}^{n} |x_i|^{r_1} \tag{18}$$

$$\left(\sum_{i=1}^{n} |x_i|\right)^{r_2} \le n^{r_2 - 1} \sum_{i=1}^{n} |x_i|^{r_2}. \tag{19}$$

Lemma 4 [42]: If $x, y \in \mathbb{R}$, $\delta > 0$, $a > 1$, $b > 1$, and $(a - 1)(b - 1) = 1$, then the following inequality holds:

$$xy \le \frac{\delta^a}{a} |x|^a + \frac{1}{b\delta^b} |y|^b. \tag{20}$$

Lemma 5 [40]: $\lambda_{\max}(M)$ and $\lambda_{\min}(M)$ represent the maximum and minimum eigenvalues of matrix M, respectively. If $\forall x \in \mathbb{R}$ and $\| \cdot \|$ stands for the Euclidean norm, then the following inequality holds:

$$\lambda_{\min}(M) \|x\|^2 \le x^T M x \le \lambda_{\max}(M) \|x\|^2. \tag{21}$$

Lemma 6 [37]: For any $l > 0$ and any $\varsigma \in \mathbb{R}$, the following inequality holds:

$$0 \le |\varsigma| - |\varsigma| \tanh\left(\frac{|\varsigma|}{l}\right) \le 0.2785 l. \tag{22}$$

Lemma 7 [31]: Consider the following NFTSM surface:

$$s = \dot{x} + K_1 S^{\alpha}(x) + K_2 \mathrm{Sig}^{\beta}(x) \tag{23}$$

where $0 < \alpha < 1$, $\beta > 1$, $K_1, K_2 \in \mathbb{R}^{n \times n}$ are positive-definite diagonal gain matrices and δ is a designed positive

Authorized licensed use limited to: CHONGQING UNIVERSITY. Downloaded on May 15,2023 at 10:16:35 UTC from IEEE Xplore. Restrictions apply.

constant. $S^{\alpha}(x)=[s^{\alpha}(x_1),s^{\alpha}(x_2),\ldots,s^{\alpha}(x_n)]^T$ and $\mathrm{Sig}^{\beta}(x)=[\mathrm{sig}^{\beta}(x_1),\mathrm{sig}^{\beta}(x_2),\ldots,\mathrm{sig}^{\beta}(x_n)]^T$

$$s^{\alpha}(x_i)=\begin{cases}|x_i|^{\alpha}\mathrm{sign}(x_i), & |x_i|\geq\delta\\ \delta^{\alpha-1}x_i, & |x_i|<\delta\end{cases}$$
$$\mathrm{sig}^{\beta}(x_i)=|x_i|^{\beta}\mathrm{sign}(x_i).$$

If $s=0$, the variable x globally converges to an arbitrary small residual set containing zero within a uniformly bounded time $T'\leq T'_{\max}=1/(K_1(1-\alpha))+1/(K_2(\beta-1))$.

III. Stability Analysis and Control Design

In this article, in order to ensure that the actual trajectory q can still track the desired trajectory q_d accurately under the conditions of external disturbance, parameter uncertainties, and input saturation within a fixed time. First, a model-based controller is designed under the assumption that the parameters are all known. However, considering that the accurate parameters are difficult to be obtained in practical applications. Then, the NNs-based controller is designed where NNs are used to approximate the compounded uncertainty.

A. Model-Based Fixed-Time Control Method

Two error variables z_1 and z_2 are defined as follows:

$$z_1=q-q_d \tag{24}$$
$$z_2=\dot{q}-\dot{q}_d. \tag{25}$$

Choose the following NFTSM surface:

$$s=z_2+K_1S^{\alpha}(z_1)+K_2\mathrm{Sig}^{\beta}(z_1) \tag{26}$$

where $0<\alpha<1$, $\beta>1$, and K_1 and K_2 are two positive-definite diagonal matrices. Then, $\dot{s}$ can be obtained as follows:

$$\begin{aligned}\dot{s}&=\dot{z}_2+\big(K_1F^{\alpha}(z_1)+K_2H^{\beta}(z_1)\big)\dot{z}_1\\&=M^{-1}(g(u)+\Delta\tau+d-C\dot{q}-g)-\ddot{q}_d\\&\quad+\big(K_1F^{\alpha}(z_1)+K_2H^{\beta}(z_1)\big)\dot{z}_1\end{aligned} \tag{27}$$

where $F^{\alpha}(x)=\mathrm{diag}[f^{\alpha}(x_1),\ldots,f^{\alpha}(x_n)]$ is the derivative of $S^{\alpha}(x)$ and $H^{\beta}(x)=\mathrm{diag}[\beta|x_1|^{\beta-1},\ldots,\beta|x_n|^{\beta-1}]$ is the derivative of $\mathrm{Sig}^{\beta}(x)$.

Construct a Lyapunov function candidate as follows:

$$V_1=\frac{1}{2}s^TMs. \tag{28}$$

Differentiating V_1, we have

$$\begin{aligned}\dot{V}_1&=s^TM\dot{s}+\frac{1}{2}s^T\dot{M}s\\&=s^T(g(u)-C\dot{q}-g-M\ddot{q}_d\\&\quad+M\big(K_1F^{\alpha}(z_1)+K_2H^{\beta}(z_1)\big)\dot{z}_1+Cs+D\big)\end{aligned} \tag{29}$$

where $D=\Delta\tau+d$. Assuming that the boundary of the disturbance $\bar{d}$ is a known constant, and then the boundary of the compounded disturbance $\bar{D}$ can be obtained, where $\bar{D}=\bar{d}+\bar{\Delta}$. In this case, the model-based controller can be designed as follows:

$$u=u_a+u_b \tag{30}$$
$$u_a=u_{a1}+u_{a2} \tag{31}$$

where

$$\begin{aligned}u_{a1}&=C\dot{q}+g+M\ddot{q}_d-M\big(K_1F^{\alpha}(z_1)+K_2H^{\beta}(z_1)\big)\dot{z}_1\\&\quad-Cs-\frac{s}{\|s\|}\left(\bar{D}\tanh\left(\frac{\bar{D}}{l}\right)+0.2785l\right)\end{aligned} \tag{32}$$

$$u_{a2}=-K_{21}\frac{s}{\|s\|^2}\left(\frac{1}{2}s^Ts\right)^{\frac{1}{2}}-K_{22}\left(\frac{1}{2}\right)^2ss^Ts \tag{33}$$

$$u_b=-\frac{\|u_a\|s}{\|s\|(1-\lambda_{\max}(\Lambda))} \tag{34}$$

where K_{21} and K_{22} are positive constants and $\lambda_{\max}(\Lambda)$ denotes the maximum eigenvalue.

Remark 2: Consider the chattering problems caused by the sign function, $s/\|s\|$ in (32) and (34) can be replaced by $s/\sqrt{\varrho_1}$, when $s^Ts<\varrho_1$ with ϱ_1 being a positive constant. For the same reason as above, the function $s/\|s\|^2$ in (33) can also encounter chattering problems. To get around this, we replace $\|s\|^2$ with ϱ_2 when $\|s\|^2<\varrho_2$ with ϱ_2 being a positive constant.

According to equation (7), we can know that $g(u)=u-\Lambda u$. Noticing the diagonal elements of Λ, we can find that $\Lambda_i\in(0,0.72)$, then the following inequality can be obtained:

$$\begin{aligned}s^Tu_b-s^T\Lambda u&=s^T(I-\Lambda)u_b-s^T\Lambda u_a\\&=-(I-\Lambda)\frac{\|u_a\|\|s\|}{1-\lambda_{\max}(\Lambda)}-s^T\Lambda u_a\\&\leq-\|u_a\|\|s\|-s^T\Lambda u_a\\&\leq 0.\end{aligned} \tag{35}$$

Substituting (30) into (29), and according to Lemmas 3, 5, and 6, it yields

$$\begin{aligned}\dot{V}_1&\leq s^TD-\|s\|\left(\bar{D}\tanh\left(\frac{\bar{D}}{l}\right)+0.2785l\right)\\&\quad-K_{21}\left(\frac{1}{2}s^Ts\right)^{\frac{1}{2}}-K_{22}\left(\frac{1}{2}s^Ts\right)^2\\&\leq-\frac{K_{21}}{\lambda_{\max}{}^{\frac{1}{2}}(M)}\left(\frac{1}{2}s^TMs\right)^{\frac{1}{2}}\\&\quad-\frac{K_{22}}{\lambda_{\max}{}^2(M)}\left(\frac{1}{2}s^TMs\right)^2.\end{aligned} \tag{36}$$

The inequality can be rewritten as follows:

$$\dot{V}_1\leq-\rho_1V_1{}^{\frac{1}{2}}-\frac{1}{2}\rho_2V_1{}^2 \tag{37}$$

where ρ_1 and ρ_2 are two positive constants given by

$$\rho_1=\frac{K_{21}}{\lambda_{\max}{}^{\frac{1}{2}}(M)} \tag{38}$$
$$\rho_2=\frac{K_{22}}{\lambda_{\max}{}^2(M)}. \tag{39}$$

Theorem 1: Suppose that the dynamic parameters of the system (1) and the boundary of the compounded disturbance are known, under Assumptions 1 and 2, applying the proposed controller (30), then the following conclusions can be obtained: 1) the sliding-mode variable s can converge to the origin within a fixed time and 2) the tracking error can also converge to the residual set within a fixed time.

Authorized licensed use limited to: CHONGQING UNIVERSITY. Downloaded on May 15,2023 at 10:16:35 UTC from IEEE Xplore. Restrictions apply.

Proof: According to (37), we can obtain

$$\dot{V}_1 \leq -\rho_1 V_1^{\frac{1}{2}} - \frac{1}{2}\rho_2 V_1^2.$$

Let $\omega = V_1^{(1/2)}$, and the derivative of ω can be expressed as follows:

$$\dot{\omega} \leq -\frac{1}{2}\left(\frac{1}{2}\rho_2\omega^3 + \rho_1\right).$$

The above inequality can be rewritten as follows:

$$\frac{d\omega}{dt} \leq -\frac{1}{2}\left(\frac{1}{2}\rho_2\omega^3 + \rho_1\right)$$
$$\frac{1}{\frac{1}{2}\rho_2\omega^3 + \rho_1}d\omega \leq -\frac{1}{2}dt.$$

Let $\varphi(\omega) = \int_0^\omega (1/[(1/2)\rho_2\omega^3 + \rho_1])d\omega$. Integrating both sides of the above inequality yields

$$\varphi(\omega(t)) \leq \varphi(\omega(0)) - \frac{1}{2}t.$$

Since $\varphi(\omega(t))$ is a monotonically increasing function, $\varphi(\omega(t)) = 0$ if and only if $\omega(t) = 0$, which implies $V_1 = 0$. The convergence time of the closed-loop system $T(V_1)$can be obtained as follows:

$$T(V_1) = 2\varphi(\omega(0)) = 2\varphi\left(V_1^{\frac{1}{2}}(0)\right).$$

Consider the case where the initial conditions for $V_1(t)$ approach infinity

$$\begin{aligned}\lim_{V_1(0)\to\infty} T(V_1(0)) &= \lim_{\omega(0)\to\infty} 2\varphi(\omega(0)) = 2\varphi(\infty)\\ &= 2\left(\int_0^1 \frac{1}{\frac{1}{2}\rho_2\omega^3 + \rho_1}d\omega + \int_1^\infty \frac{1}{\frac{1}{2}\rho_2\omega^3 + \rho_1}d\omega\right)\\ &< 2\left(\int_0^1 \frac{1}{\rho_1}d\omega + \int_1^\infty \frac{1}{\frac{1}{2}\rho_2\omega^3}d\omega\right)\\ &= \frac{2}{\rho_1} + \frac{2}{\rho_2} = T_{\max}. \end{aligned} \tag{40}$$

According to (40), it can be found that the signal s can converge to the origin within a fixed time $T_{\max}$. The time of the tracking errors sliding on the sliding surface depends on the design of the sliding surface. According to Lemma 7, the convergence time of the tracking errors on the sliding surface is bounded by $T'_{\max}$. Therefore, the object of this article is to ensure that the convergence time of sliding-mode variables is uniformly bounded. ■

Remark 3: It can be found intuitively that the upper bound of convergence time is independent of the initial conditions. Even if the initial conditions approach infinity, the upper bound of the convergence time of the system does not change. In order to deal with the problem of input saturation, the input is transformed into a new form. According to (34), it can be found that u_b is designed based on u_a and the result of (35) is always valid no matter what u_a is. Consequently, the designer only needs to focus on the design of u_a.

B. NNs-Based Fixed-Time Control Method

In this section, the kinetic parameters M, C, and G and the boundary of compound disturbance are assumed to be unknown for the reason of imprecise system parameters in practical applications. To solve this problem, the unknown dynamics of the system and the unknown compound disturbance are integrated into the compound uncertainties, which can be approximated by RBFNNs

$$\begin{aligned}W^{*T}S(X) + \varepsilon = Cs + M\big(K_1F^\alpha(z_1) + K_2H^\beta(z_1)\big)\dot{z}_1\\ - C\dot{q} - g - M\ddot{q}_d + D\end{aligned} \tag{41}$$

where $X = [q^T, \dot{q}^T, q_d^T, \dot{q}_d^T, \ddot{q}_d^T, s^T]^T$ denotes the input of RBFNNs and ε denotes the approximate error which satisfies $\|\varepsilon(t)\| \leq \bar{\varepsilon}$. $\bar{\varepsilon}$ is an unknown positive constant and D denotes the unknown compound disturbance.

The controller is given as follows:

$$\begin{aligned}u_a = -K_{21}\frac{s}{\|s\|^2}\left(\frac{1}{2}s^Ts\right)^{\frac{1}{2}} - K_{22}\left(\frac{1}{2}\right)^2 ss^Ts\\ - \hat{W}^TS(X) - \frac{1}{2}s\end{aligned} \tag{42}$$

where $\hat{W}$ represents the estimate of the ideal weight. Then, the adaptive law is formulated as follows:

$$\dot{\hat{W}}_i = -\Gamma_{2i}\hat{W}_i\hat{W}_i^T\hat{W}_i + \Gamma_{2i}S_i(X)s_i \tag{43}$$

where the controller parameter Γ_{2i} is a positive-definite diagonal gain matrix.

Define $\tilde{W}_i = \hat{W}_i - W_i{}^*$ and choose a Lyapunov function as follows:

$$V_2 = \frac{1}{2}\sum_{i=1}^n \tilde{W}_i^T\Gamma_{2i}^{-1}\tilde{W}_i. \tag{44}$$

Substituting the adaptive law (43) into the derivative of (44)

$$\begin{aligned}\dot{V}_2 &= \sum_{i=1}^n \tilde{W}_i^T\Gamma_{2i}^{-1}\dot{\hat{W}}_i\\ &\leq -\sum_{i=1}^n \tilde{W}_i^T\hat{W}_i\hat{W}_i^T\hat{W}_i + \sum_{i=1}^n \tilde{W}_i^TS_i(X)s_i\\ &\leq -\sum_{i=1}^n \|\tilde{W}_i\|^4 - \sum_{i=1}^n \|W_i{}^*\|^2\left(\|\tilde{W}_i\|^2 + \tilde{W}_i^TW_i{}^*\right)\\ &\quad - 3\sum_{i=1}^n \|\tilde{W}_i\|^2\tilde{W}_i^TW_i{}^* - 2\sum_{i=1}^n \|\tilde{W}_i^TW_i{}^*\|^2\\ &\quad + \sum_{i=1}^n \tilde{W}_i^TS_i(X)s_i. \end{aligned} \tag{45}$$

According to Lemma 4, the following inequalities are proposed:

$$\begin{aligned}-3\|\tilde{W}_i\|^2\tilde{W}_i^TW_i{}^* &\leq 3\|\tilde{W}_i\|^3\|W_i{}^*\|\\ &\leq \frac{9}{4}k_{1i}^{\frac{4}{3}}\left(\|\tilde{W}_i\|^3\right)^{\frac{4}{3}} + \frac{3}{4k_{1i}^4}\|W_i{}^*\|^4\\ -\|W_i{}^*\|^2\tilde{W}_i^TW_i{}^* &\leq \|W_i{}^*\|^3\|\tilde{W}_i\|\end{aligned}$$

Authorized licensed use limited to: CHONGQING UNIVERSITY. Downloaded on May 15,2023 at 10:16:35 UTC from IEEE Xplore. Restrictions apply.

$$\leq \frac{3}{4}k_{2i}{}^{\frac{4}{3}}\left(\|W_i{}^*\|^3\right)^{\frac{4}{3}} + \frac{1}{4k_{2i}{}^4}\|\tilde{W}_i\|^4$$
$$-\|W_i{}^*\|^2\|\tilde{W}_i\|^2 \leq -\|W_i{}^*\|^2\left(2\|\tilde{W}_i\| - 1\right).$$

Therefore, the following inequality can be obtained as follows:

$$\dot{V}_2 \leq -\sum_{i=1}^{n}\left(1 - \frac{9}{4}k_{1i}{}^{\frac{4}{3}} - \frac{1}{4k_{2i}{}^4}\right)\|\tilde{W}_i\|^4 - 2\sum_{i=1}^{n}\|W_i{}^*\|^2\|\tilde{W}_i\| + \sum_{i=1}^{n}\tilde{W}_i^T S_i(X)s_i + \zeta_1 \quad (46)$$

$$\zeta_1 = \sum_{i=1}^{n}\left(\frac{3}{4k_{1i}{}^4} + \frac{3}{4}k_{2i}{}^{\frac{4}{3}}\right)\|W_i{}^*\|^4 + \sum_{i=1}^{n}\|W_i{}^*\|^2. \quad (47)$$

Redefine a positive-definite Lyapunov function of the following form:

$$V_3 = V_1 + V_2. \quad (48)$$

Considering (28) and (44), the following inequality can be gained:

$$\dot{V}_3 \leq -K_{21}{}^*\left(\frac{1}{2}s^T M s\right)^{\frac{1}{2}} - K_{22}{}^*\left(\frac{1}{2}s^T M s\right)^2 - K_{31}\sum_{i=1}^{n}\left(\frac{1}{2}\tilde{W}_i^T\Gamma_{2i}^{-1}\tilde{W}_i\right)^{\frac{1}{2}} - K_{32}\sum_{i=1}^{n}\left(\frac{1}{2}\tilde{W}_i^T\Gamma_{2i}^{-1}\tilde{W}_i\right)^2 + \zeta \quad (49)$$

where

$$K_{21}{}^* = \frac{K_{21}}{\lambda_{\max}{}^{\frac{1}{2}}(M)} \quad (50)$$

$$K_{22}{}^* = \frac{K_{22}}{\lambda_{\max}{}^2(M)} \quad (51)$$

$$K_{31} = \min_{i=1,2,\ldots,n}\frac{2\sqrt{2}\|W_i{}^*\|^2}{\lambda_{\max}{}^{\frac{1}{2}}\left(\Gamma_{2i}^{-1}\right)} \quad (52)$$

$$K_{32} = \min_{i=1,2,\ldots,n}\frac{4\left(1 - \frac{9}{4}k_{1i}{}^{\frac{4}{3}} - \frac{1}{4k_{2i}{}^4}\right)}{\lambda_{\max}{}^2\left(\Gamma_{2i}^{-1}\right)} \quad (53)$$

$$\zeta = \sum_{i=1}^{n}\left(\frac{3}{4k_{1i}{}^4} + \frac{3}{4}k_{2i}{}^{\frac{4}{3}}\right)\|W_i{}^*\|^4 + \sum_{i=1}^{n}\|W_i{}^*\|^2 + \frac{1}{2}\bar{\varepsilon}^2. \quad (54)$$

Then, the following formulation can be obtained:

$$\dot{V}_3 \leq -\rho_3 V_3{}^{\frac{1}{2}} - \frac{1}{n+1}\rho_4 V_3{}^2 + \zeta \quad (55)$$

where n represents the number of W_i, and ρ_3 and ρ_4 are given as follows:

$$\rho_3 = \min\left(\frac{K_{21}}{\lambda_{\max}{}^{\frac{1}{2}}(M)}, K_{31}\right) \quad (56)$$

$$\rho_4 = \min\left(\frac{K_{22}}{\lambda_{\max}{}^2(M)}, K_{32}\right). \quad (57)$$

According to Lemma 2, the convergence time of the variables s and $\tilde{W}$ is bounded by

$$T \leq T_{\max} = \frac{2}{v\rho_3} + \frac{n+1}{v\rho_4}. \quad (58)$$

Theorem 2: Consider the system (1) subject to external disturbances, unknown dynamics, and input saturation, under the controller (34), (42) and the NNs adaption law (43), the following conclusions can be obtained: 1) the variables s and $\tilde{W}$ can enter into a residual set Ω_x within a fixed time and 2) the convergence time of the tracking errors is also uniformly bounded.

Proof: According to (55), we can obtain

$$\dot{V}_3 \leq -\rho_3 V_3{}^{\frac{1}{2}} - \frac{1}{n+1}\rho_4 V_3{}^2 + \zeta.$$

Introducing a constant $0 < v < 1$, and the above inequality can be rewritten as follows:

$$\dot{V}_3 \leq -v\rho_3 V_3{}^{\frac{1}{2}} - (1-v)\rho_3 V_3{}^{\frac{1}{2}} - \frac{\rho_4}{n+1}V_3{}^2 + \zeta$$

or

$$\dot{V}_3 \leq -\rho_3 V_3{}^{\frac{1}{2}} - \frac{v}{n+1}\rho_4 V_3{}^2 - \frac{(1-v)\rho_4}{n+1}V_3{}^2 + \zeta.$$

In the first case, if $V_3 > (\zeta/[(1-v)\rho_3])^2$, the following inequality can be given as follows:

$$\dot{V}_3 \leq -v\rho_3 V_3{}^{\frac{1}{2}} - \frac{\rho_4}{n+1}V_3{}^2.$$

According to Lemma 1, the following results can be obtained:

$$x \in \left\{V_3(x) \leq \left(\frac{\zeta}{(1-v)\rho_3}\right)^2\right\}$$

and the convergence time is bounded by

$$T \leq T_{\max} = \frac{2}{v\rho_3} + \frac{n+1}{\rho_4}.$$

In the second case, if $V_3 > ([(n+1)\zeta]/[(1-v)\rho_4])^{(1/2)}$, the following inequality can be given as follows:

$$\dot{V}_3 \leq -\rho_3 V_3{}^{\frac{1}{2}} - \frac{v\rho_4}{n+1}V_3{}^2.$$

According to Lemma 1, the following results can be obtained:

$$x \in \left\{V_3(x) \leq \left(\frac{(n+1)\zeta}{(1-v)\rho_4}\right)^{\frac{1}{2}}\right\}$$

and the convergence time is bounded by

$$T \leq T_{\max} = \frac{2}{\rho_3} + \frac{n+1}{v\rho_4}.$$

The conclusion in Theorem 2 can be proved by combining the two cases. The convergent residual set is shown as follows:

$$\Omega_x = \left\{x | V(x) \leq \min\left\{\left[\frac{(n+1)\zeta}{\rho_4(1-v)}\right]^{\frac{1}{2}}, \left[\frac{\zeta}{\rho_3(1-v)}\right]^2\right\}\right\}. \quad (59)$$

Authorized licensed use limited to: CHONGQING UNIVERSITY. Downloaded on May 15,2023 at 10:16:35 UTC from IEEE Xplore. Restrictions apply.

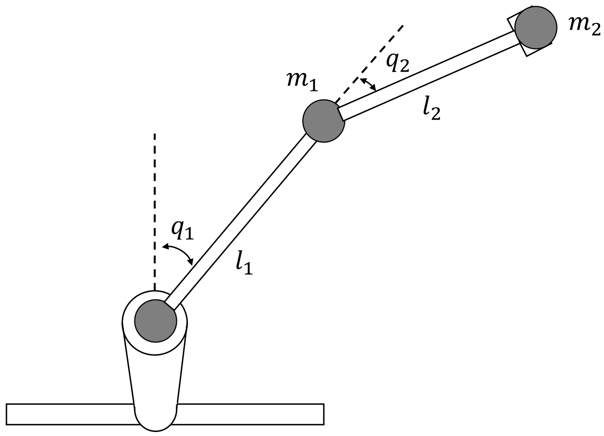

Fig. 1. Diagram of the two-link robotic manipulator.

According to Lemma 2, it can be found that V_3 is practical fixed-time stable, and $x = [s^T, \tilde{W}_i]$ will ultimately converge to the residual set Ω_x within the period $T_{\max}$. Therefore, Theorem 2 is proved. It is worth noting that different from fixed-time stability, the practical fixed-time stability means that the states converge to a residual set within a fixed time, while fixed-time stability means that the states can converge to zero. ■

Remark 4: Compared with the model-based control method, the NN-based sliding-mode control method does not need to obtain accurate system models, which is hard to be available in practice. Therefore, the proposed control method has a wider application range.

Remark 5: Theoretically speaking, we can shorten the upper bound of convergence time by increasing the values of the K_{21}, K_{22}, and Γ_{2i}, and the result is that the amplitude of the input will also increase. To ensure that the robotic system can achieve stable trajectory tracking within a fixed time, the crucial premise is that the actuators can still produce sufficient actuating torques to drive the system even if there exists the upper amplitude of the actuators [43]. The selection of design parameters needs to take into account the upper bound of the actuator amplitude, so the parameters can be determined by the trial-and-error method.

IV. Simulation

In this part, a comparative simulation based on the two-link rigid robotic manipulator is conducted to verify the effectiveness of the controller designed in Section III. The simplified plane diagram structure of the two-link manipulator is shown in Fig. 1 and the position vector q can be rewritten as follows:

$$q = \begin{bmatrix} q_1 & q_2 \end{bmatrix}^T. \tag{60}$$

The dynamics model (1) is defined by

$$\begin{aligned} M(q) &= \begin{bmatrix} p_1 + 2p_2\cos(q_2) & p_3 + p_2\cos(q_2) \\ p_3 + p_2\cos(q_2) & p_4 \end{bmatrix} \\ C(q,\dot{q}) &= \begin{bmatrix} -p_2\sin(q_2)\dot{q}_2 & -2p_2\sin(q_2)\dot{q}_2 \\ p_2\sin(q_2)\dot{q}_1 & 0 \end{bmatrix} \\ g(q) &= \begin{bmatrix} p_5\cos(q_1) + p_6\cos(q_1+q_2) \\ p_6\cos(q_1+q_2) \end{bmatrix} \end{aligned} \tag{61}$$

TABLE I
System Parameters

Parameter	Description	Value
m_1	Mass of link 1	0.5 kg
m_2	Mass of link 2	1.5 kg
l_1	Length of link 1	1.0 m
l_2	Length of link 2	0.8 m
J_1	Inertia of link 1	5.0 kgm^2
J_2	Inertia of link 2	5.0 kgm^2

where

$$\begin{aligned} p_1 &= (m_1+m_2){l_1}^2 + m_2{l_2}^2 + J_1 \\ p_2 &= m_2 l_1 l_2 \\ p_3 &= m_2{l_2}^2 \\ p_4 &= p_3 + J_2 \\ p_5 &= (m_1+m_2)l_1 g \\ p_6 &= m_2 l_2 g. \end{aligned} \tag{62}$$

In order to verify the effectiveness of the proposed method for tracking control of the manipulator system with parameter perturbation, a Monte Carlo simulation is employed to verify the robustness of the proposed method. The nominal parameters of the manipulator are shown in Table I. Define the actual mass of the link 1 $m_1' = m_1 + \Delta m_1$ and the actual mass of the link 2 $m_2' = m_2 + \Delta m_2$, where $\Delta m_1 \in [-0.1, 0.1]$ and $\Delta m_2 \in [-0.3, 0.3]$ are random numbers. Similarly, define the actual length of the link 1 $l_1' = l_1 + \Delta l_1$ and the actual length of the link 2 $l_2' = l_2 + \Delta l_2$, where $\Delta l_1 \in [-0.2, 0.2]$ and $\Delta l_2 \in [-0.16, 0.16]$ are also random numbers. The cycle times of the entire simulation are set as 100 times, and the average value of the total output is taken as the actual output. The initial values of the manipulator are specified as $q_1(0) = 1$, $q_2(0) = 1.5$, $\dot{q}_1(0) = 0$, and $\dot{q}_2(0) = 0$. The desired tracking trajectory is given as follows:

$$q_d = \begin{bmatrix} 1.25 - 1.4e^{-t} + 0.35e^{-4t} \\ 1.25 + e^{-t} + 0.25e^{-4t} \end{bmatrix} \tag{63}$$

where $t \in [0, t_f]$ and $t_f = 10$ s. The external disturbance vector simulated is of the form

$$d = \begin{bmatrix} 2\sin(t) + 0.5\sin(200\pi t) \\ \cos(2t) + 0.5\sin(200\pi t) \end{bmatrix}. \tag{64}$$

To proceed with the design of robust adaptive fixed-time sliding-mode control scheme, all design parameters are chosen as $\alpha = 0.5$, $\beta = 2.5$, $K_1 = \mathrm{diag}\{5, 5\}$, $K_2 = \mathrm{diag}\{5, 5\}$, $K_{21} = 50$, and $K_{22} = 40$. Practically, actuators have an upper bound on the amplitude and the upper amplitude of the actuator set to $\tau_{\max} = [150, 150]^T$ Nm. The input saturation parameter is chosen as $\lambda_{\max}(\Lambda) = 0.72$. For the NNs-based control, $\Gamma_{21} = 100I_{256\times256}$ and $\Gamma_{22} = 100I_{256\times256}$. An RBFNN $W^T S(X)$ contains 256 nodes with centers spaced evenly in the interval $[-3, 3] \times [-3, 3] \times [-3, 3] \times [-3, 3] \times [-3, 3] \times [-3, 3] \times [-3, 3] \times [-3, 3] \times [-3, 3] \times [-3, 3] \times [-3, 3] \times [-3, 3]$ and the value of width is 8.

Simulation results under the proposed scheme are shown in Figs. 2–7. The position tracking performances and trajectory errors of q_1 and q_2 are shown in Figs. 2 and 3, respectively.

Authorized licensed use limited to: CHONGQING UNIVERSITY. Downloaded on May 15,2023 at 10:16:35 UTC from IEEE Xplore. Restrictions apply.

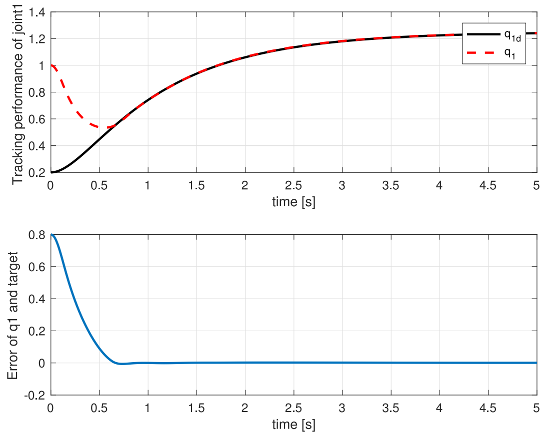

Fig. 2. Tracking performance and error of q_1 with NNs-based fixed-time control.

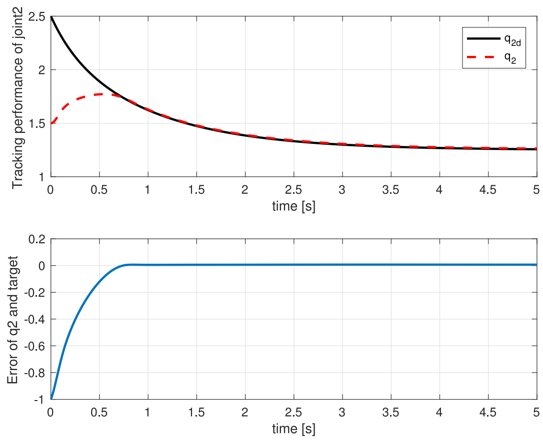

Fig. 3. Tracking performance and error of q_2 with NNs-based fixed-time control.

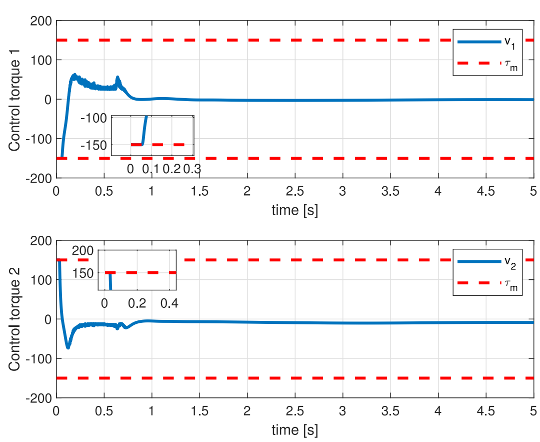

Fig. 4. NNs-based fixed-time control input.

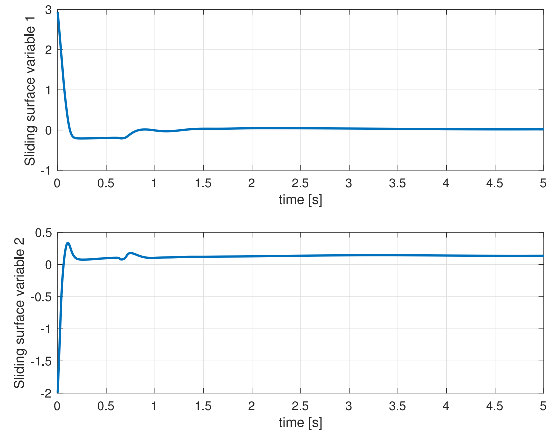

Fig. 5. NNs-based fixed-time sliding surface function.

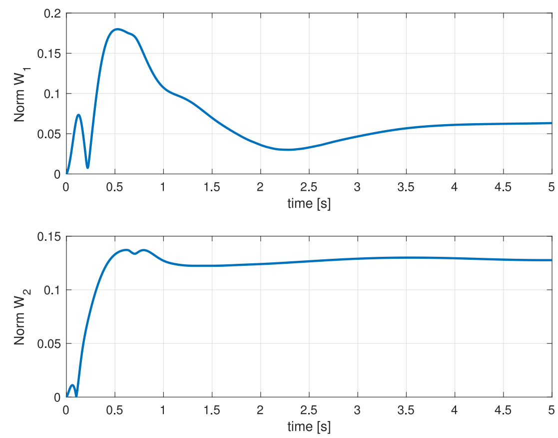

Fig. 6. Estimation weights with NNs-based fixed-time control.

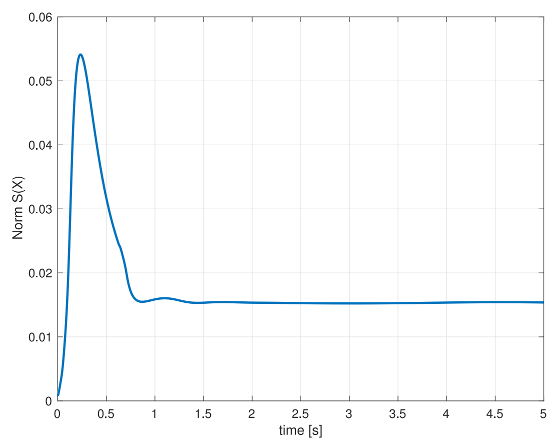

Fig. 7. Norm of the Gaussian function.

Figs. 2 and 3 indicate that the developed scheme can make the actual position q track the desired trajectory q_d with satisfactory performance. The control input is shown in Fig. 4. It can be observed from Fig. 4 that the input constraint is not violated and the problem of control chattering is solved simultaneously. According to Fig. 5, it is clear that the sliding surface functions converge to the residual set around zero. The norm of NNs weights can be noticed in Fig. 6 and the norm of the Gaussian function can be observed in Fig. 7.

To further illuminate the superiority of the proposed control scheme in this article, a simulation comparison with the finite-time NFTSMC scheme in [26] is carried out. The NFTSMC law is given as follows:

$$\begin{aligned}
\tau_{eq} &= M\ddot{q}_d + C\dot{q} + G - \frac{M}{\beta}|z_2|^{2-\beta}\left(1 + \alpha|z_1|^{\alpha-1}\right)\mathrm{sign}(z_2) \\
\tau_{sw} &= -M\big[ks + (\delta + \eta)\mathrm{sign}(s)\big] \\
\tau &= \tau_{eq} + \tau_{sw} \\
s &= z_1 + |z_1|^{\alpha}\mathrm{sign}(z_1) + |z_2|^{\beta}\mathrm{sign}(z_2)
\end{aligned}$$

Authorized licensed use limited to: CHONGQING UNIVERSITY. Downloaded on May 15,2023 at 10:16:35 UTC from IEEE Xplore. Restrictions apply.

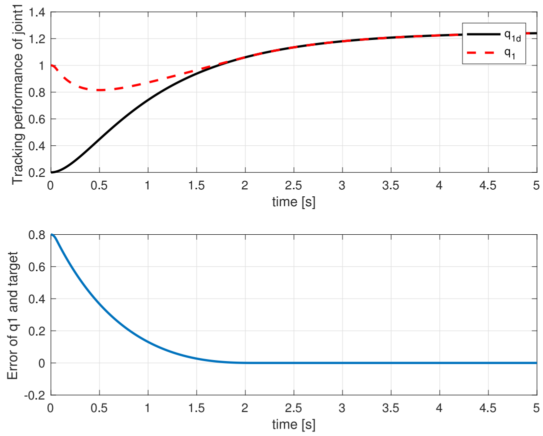

Fig. 8. Tracking performance and error of q_1 with finite-time NFTSMC.

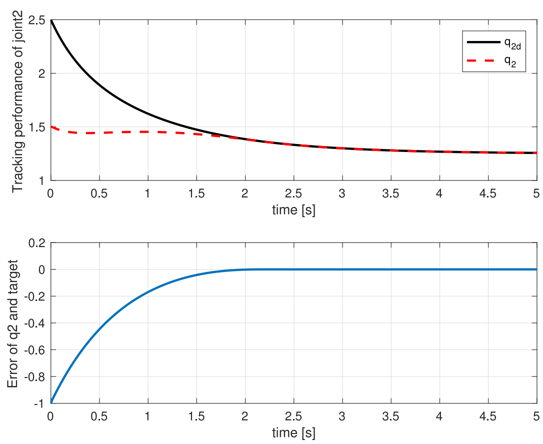

Fig. 9. Tracking performance and error of q_2 with finite-time NFTSMC.

where $\alpha = 2$, $\beta = 5/3$, $\eta = 0.5$, $k = 50$, and $\delta = 2.5$ denotes the upper boundary of the external disturbance. s represents the NFTSMC surface. In order to make the comparison fair, the system parameters M, C, and G are consistent with the parameters in this article. According to Figs. 8 and 9, it can be found that the convergence time of the method proposed in [26] is obviously larger than that of the method proposed in this article. What is more, as we can see from Fig. 10 that the chattering problem is serious.

Furthermore, we reset the initial conditions as $q(0) = [2\ \ 1]^T$ and $[3\ \ 0.5]^T$, and other design parameters remain unchanged. It can be observed from Figs. 11 and 12 that the convergence time of the method proposed in [26] increases with the increase of the initial tracking errors. However, our fixed-time method does not have this phenomenon. Therefore, according to comparison results, we can conclude that the convergence time of the state variable in this article is independent of the initial conditions.

V. Conclusion

In this article, a robust adaptive fixed-time sliding-mode controller has been proposed for a class of robotic systems with external disturbance, unknown dynamics, and input saturation. A model-based fixed-time controller is designed

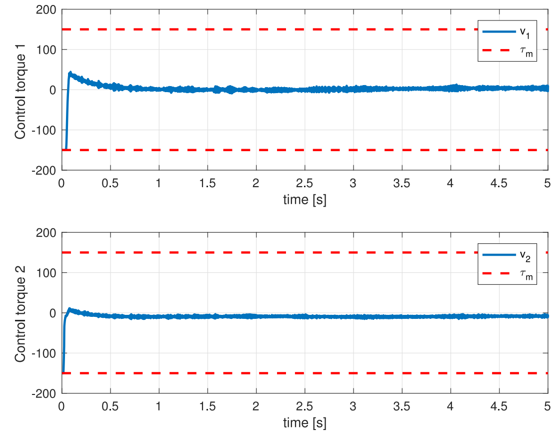

Fig. 10. Finite-time NFTSMC input.

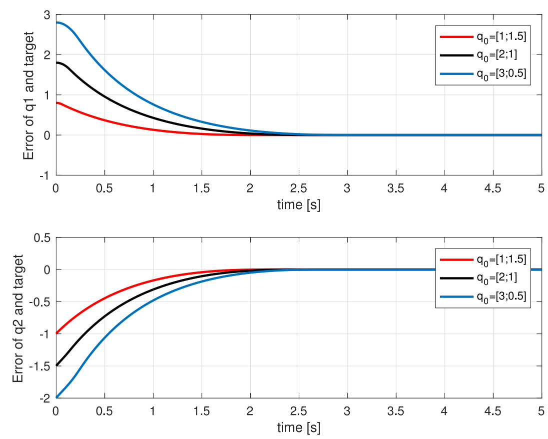

Fig. 11. Finite-time NFTSMC tracking errors with different initial conditions.

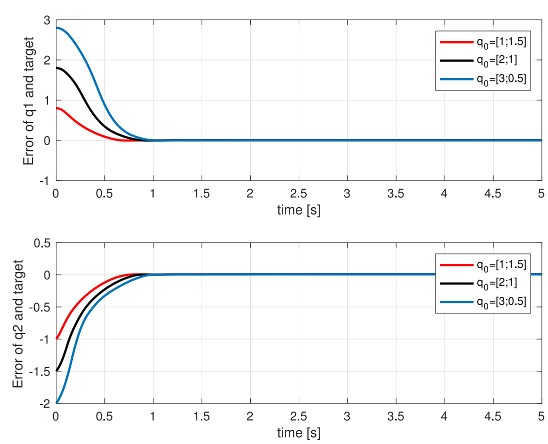

Fig. 12. NNs-based fixed-time tracking errors with different initial conditions.

supposing that the system parameters and upper boundary of disturbance are known. In order to enhance the robustness and convergence speed of the system, NFTSM has been applied in the controller design. Then, considering the situation that the upper boundary of disturbance is not available, the unknown dynamics of robotic systems and the boundary of compounded disturbance are synthesized into a compounded uncertainty which is approximated by an adaptive NNs. Furthermore, the input constraint is not violated and the problem of control

Authorized licensed use limited to: CHONGQING UNIVERSITY. Downloaded on May 15,2023 at 10:16:35 UTC from IEEE Xplore. Restrictions apply.

chattering is solved. The simulation results show that the deviation variables can converge to a residual set containing zero within a fixed time and verify the superior performance of the proposed methods. Future directions will consider how to combine fault-tolerant control with fixed-time control in high-order uncertain nonlinear systems.

REFERENCES

[1] P. Kebria, A. Khosravi, S. Nahavandi, P. Shi, and R. Alizadehsani, "Robust adaptive control scheme for teleoperation systems with delay and uncertainties," *IEEE Trans. Cybern.*, vol. 50, no. 7, pp. 3243–3253, Jul. 2020.

[2] H. Li, S. Zhao, W. He, and R. Lu, "Adaptive finite-time tracking control of full state constrained nonlinear systems with dead-zone," *Automatica*, vol. 100, pp. 99–107, Feb. 2019.

[3] B. Qin, H. Yan, H. Zhang, Y. Wang, and S. X. Yang, "Enhanced reduced-order extended state observer for motion control of differential driven mobile robot," *IEEE Trans. Cybern.*, early access, Nov. 30, 2021, doi: 10.1109/TCYB.2021.3123563.

[4] Z. Li, W. Yuan, Y. Chen, F. Ke, X. Chu, and C. Chen, "Neural-dynamic optimization-based model predictive control for tracking and formation of nonholonomic multirobot systems," *IEEE Trans. Neural Netw. Learn. Syst.*, vol. 29, no. 12, pp. 6113–6122, Dec. 2018.

[5] Y. Chen, Z. Li, H. Kong, and F. Ke, "Model predictive tracking control of nonholonomic mobile robots with coupled input constraints and unknown dynamics," *IEEE Trans. Ind. Informat.*, vol. 15, no. 6, pp. 3196–3205, Jun. 2019.

[6] Z. Shen, Y. Ma, and Y. Song, "Robust adaptive fault-tolerant control of mobile robots with varying center of mass," *IEEE Trans. Ind. Electron.*, vol. 65, no. 3, pp. 2419–2428, Mar. 2018.

[7] M. Van, M. Mavrovouniotis, and S. Ge, "An adaptive backstepping nonsingular fast terminal sliding mode control for robust fault tolerant control of robot manipulators," *IEEE Trans. Syst., Man, Cybern., Syst.*, vol. 49, no. 7, pp. 1448–1458, Jul. 2019.

[8] G. Wen, Y. Liu, and Z. Liu, "Observer-based adaptive backstepping consensus tracking control for high-order nonlinear semi-strict-feedback multiagent systems," *IEEE Trans. Cybern.*, vol. 46, no. 7, pp. 1591–1601, Jul. 2016.

[9] C. Yang, Y. Jiang, J. Na, Z. Li, L. Cheng, and C. Su, "Finite-time convergence adaptive fuzzy control for dual-arm robot with unknown kinematics and dynamics," *IEEE Trans. Fuzzy Syst.*, vol. 27, no. 3, pp. 574–588, Mar. 2019.

[10] Y. Wang, H. Yan, H. Zhang, H. Shen, and H. -K. Lam, "Interval type-2 fuzzy control for HMM-based multiagent systems via dynamic event-triggered scheme," *IEEE Trans. Fuzzy Syst.*, early access, Aug. 4, 2021, doi: 10.1109/TFUZZ.2021.3101581.

[11] C.-J. Juang, M.-G. Lai, and W.-T. Zeng, "Evolutionary fuzzy control and navigation for two wheeled robots cooperatively carrying an object in unknown environments," *IEEE Trans. Cybern.*, vol. 45, no. 9, pp. 1731–1743, Sep. 2015.

[12] J. Huang, M. Ri, D. Wu, and S. Ri, "Interval type-2 fuzzy logic modeling and control of a mobile two-wheeled inverted pendulum," *IEEE Trans. Fuzzy Syst.*, vol. 26, no. 4, pp. 2030–2038, Aug. 2018.

[13] M. Xue, H. Yan, H. Zhang, X. Zhan, and K. Shi, "Compensation-based output feedback control for fuzzy markov jump systems with random packet losses," *IEEE Trans. Cybern.*, early access, Aug. 10, 2021, doi: 10.1109/TCYB.2021.3088872.

[14] M. Chen, H. Yan, H. Zhang, M. Chi, and Z. Li, "Dynamic event-triggered asynchronous control for nonlinear multiagent systems based on T-S fuzzy models," *IEEE Trans. Fuzzy Syst.*, vol. 29, no. 9, pp. 2580–2592, Sep. 2021.

[15] J. Baek, M. Jin, and S. Han, "A new adaptive sliding-mode control scheme for application to robot manipulators," *IEEE Trans. Ind. Electron.*, vol. 63, no. 6, pp. 3628–3637, Jun. 2016.

[16] Y. X. Su and C. H. Zheng, "A new nonsingular integral terminal sliding mode control for robot manipulators," *Int. J. Syst. Sci.*, vol. 51, no. 8, pp. 1418–1428, Jun. 2020.

[17] J. Lee, P. Chang, and M. Jin, "Adaptive integral sliding mode control with time-delay estimation for robot manipulators," *IEEE Trans. Ind. Electron.*, vol. 64, no. 8, pp. 6796–6804, Aug. 2017.

[18] H. Yan, X. Zhou, H. Zhang, F. Yang, and Z. -G. Wu, "A novel sliding mode estimation for microgrid control with communication time delays," *IEEE Trans. Smart Grid*, vol. 10, no. 2, pp. 1509–1520, Mar. 2019.

[19] D. Chen and Y. Zhang, "Robust zeroing neural-dynamics and its time-varying disturbances suppression model applied to mobile robot manipulators," *IEEE Trans. Neural Netw. Learn. Syst.*, vol. 29, no. 9, pp. 4385–4397, Sep. 2018.

[20] W. He and Y. Dong, "Adaptive fuzzy neural network control for a constrained robot using impedance learning," *IEEE Trans. Neural Netw. Learn. Syst.*, vol. 29, no. 4, pp. 1174–1186, Apr. 2018.

[21] V. Narayanan, S. Jagannathan, and K. Ramkumar, "Event-sampled output feedback control of robot manipulators using neural networks," *IEEE Trans. Neural Netw. Learn. Syst.*, vol. 30, no. 6, pp. 1651–1658, Jun. 2019.

[22] Z. Y. Chen, X. Yang, and X. Liu, "RBFNN-based nonsingular fast terminal sliding mode control for robotic manipulators including actuator dynamics," *Neurocomputing*, vol. 362, pp. 72–82, Oct. 2019.

[23] Z.-G. Wu, P. Shi, H. Su, and J. Chu, "Local synchronization of chaotic neural networks with sampled-data and saturating actuators," *IEEE Trans. Cybern.*, vol. 44, no. 12, pp. 2635–2645, Dec. 2014.

[24] L. Zhang, L. Liu, Z. Wang, and Y. Xia, "Continuous finite-time control for uncertain robot manipulators with integral sliding mode," *IET Control Theroy Appl.*, vol. 12, no. 11, pp. 1621–1627, 2018.

[25] Y. Feng, X. Yu, and Z. Man, "Non-singular terminal sliding mode control of rigid manipulators," *Automatica*, vol. 38, no. 12, pp. 2159–2167, 2002.

[26] M. Boukattaya, N. Mezghani, and T. Damak, "Adaptive nonsingular fast terminal sliding-mode control for the tracking problem of uncertain dynamical systems," *ISA Trans.*, vol. 77, pp. 1–19, Jun. 2018.

[27] A. Polyakov, "Nonlinear feedback design for fixed-time stabilization of linear control systems," *IEEE Trans. Autom. Control*, vol. 57, no. 8, pp. 2106–2110, Aug. 2012.

[28] A. Polyakov, D. Efimov, and W. Perruquetti, "Finite-time and fixed-time stabilization: Implicit Lyapunov function approach," *Automatica*, vol. 51, pp. 332–340, Jan. 2015.

[29] Z. Zuo, "Nonsingular fixed-time consensus tracking for second-order multi-agent networks," *Automatica*, vol. 54, pp. 305–309, Apr. 2015.

[30] S. Shi, J. Gu, S. Xu, and H. Min, "Globally fixed-time high-order sliding mode control for new sliding mode systems subject to mismatched terms and its application," *IEEE Trans. Ind. Electron.*, vol. 67, no. 12, pp. 10776–10786, Dec. 2020.

[31] Y. Su, C. Zheng, and P. Mercorelli, "Robust approximate fixed-time tracking control for uncertain robot manipulators," *Mech. Syst. Signal Process.*, vol. 135, Jan. 2020, Art. no. 106379.

[32] Y. Yang, "A time-specified nonsingular terminal sliding mode control approach for trajectory tracking of robotic airships," *Nonlinear Dyn.*, vol. 92, no. 3, pp. 1359–1367, 2018.

[33] S. Zhang, P. Yang, L. Kong, W. Chen, Q. Fu, and K. Peng, "Neural networks-based fault tolerant control of a robot via fast terminal sliding mode," *IEEE Trans. Syst., Man, Cybern., Syst.*, vol. 51, no. 7, pp. 4091–4101, Jul. 2021, doi: 10.1109/TSMC.2019.2933050.

[34] H. Wang, P. Shi, H. Li, and Q. Zhou, "Adaptive neural tracking control for a class of nonlinear systems with dynamic uncertainties," *IEEE Trans. Cybern.*, vol. 47, no. 10, pp. 3075–3087, Oct. 2017.

[35] D. Zhang, L. Kong, S. Zhang, Q. Li, and Q. Fu, "Neural networks-based fixed-time control for a robot with uncertainties and input deadzone," *Neurocomputing*, vol. 390, pp. 139–147, May 2020.

[36] Y. Yang, "Positioning control for stratospheric satellites subject to dynamics uncertainty and input constraints," *Aerosp. Sci. Technol.*, vol. 86, pp. 534–541, Mar. 2019.

[37] G. Zhu and J. Du, "Robust adaptive neural practical fixed-time tracking control for uncertain Euler-Lagrange systems under input saturations," *Neurocomputing*, vol. 412, pp. 502–513, Oct. 2020.

[38] Y.-J. Liu and S. Tong, "Barrier Lyapunov functions-based adaptive control for a class of nonlinear pure-feedback systems with full state constraints," *Automatica*, vol. 64, pp. 70–75, Feb. 2016.

[39] M. Chen, G. Tao, and B. Jiang, "Dynamic surface control using neural networks for a class of uncertain nonlinear systems with input saturation," *IEEE Trans. Neural Netw. Learn. Syst.*, vol. 26, no. 9, pp. 2086–2097, Sep. 2015.

[40] Z. Zuo, B. Tian, M. Defoort, and Z. Ding, "Fixed-time consensus tracking for multi-agent systems with high-order integrator dynamics," *IEEE Trans. Autom. Control*, vol. 63, no. 2, pp. 563–570, Feb. 2018.

[41] Z. Zheng, M. Feroskhan, and L. Sun, "Adaptive fixed-time trajectory tracking control of a stratospheric airship," *ISA Trans.*, vol. 76, pp. 134–144, May 2018.

[42] H. Wang, B. Chen, and C. Lin, "Adaptive neural tracking control for a class of stochastic nonlinear systems," *Int. J. Robust Nonlinear Control*, vol. 24, no. 7, pp. 1262–1280, 2014.

Authorized licensed use limited to: CHONGQING UNIVERSITY. Downloaded on May 15,2023 at 10:16:35 UTC from IEEE Xplore. Restrictions apply.

[43] Q. Hu, X. Shao, and W.-H. Chen, "Adaptive fault-tolerant attitude tracking control of spacecraft with prescribed performance," *IEEE/ASME Trans. Mechatronics*, vol. 23, no. 1, pp. 331–341, Feb. 2018.

[44] L. Wang, Z. Zeng, and M.-F. Ge, "A disturbance rejection framework for finite-time and fixed-time stabilization of delayed memristive neural networks," *IEEE Trans. Syst., Man, Cybern., Syst.*, vol. 51, no. 2, pp. 905–915, Feb. 2021.

Yunsong Hu received the B.S. degree in automation from the Jiangsu University of Science and Technology, Zhenjiang, Jiangsu, China, in 2019. He is currently pursuing the Ph.D. degree in control science and engineering with the East China University of Science and Technology, Shanghai, China.

His current research interests include fault-tolerant control, networked control systems, and robotics.

Huaicheng Yan received the B.Sc. degree in automatic control from the Wuhan University of Technology, Wuhan, China, in 2001, and the Ph.D. degree in control theory and control engineering from the Huazhong University of Science and Technology, Wuhan, in 2007.

In 2011, he was a Research Fellow with the University of Hong Kong, Hong Kong, for three months, and also a Research Fellow with the City University of Hong Kong, Hong Kong, in 2012, for six months. He is currently a Professor with the Key Laboratory of Smart Manufacturing in Energy Chemical Process of Ministry of Education, East China University of Science and Technology, Shanghai, China, and also with the School of Information Science and Engineering, Chengdu University, Chengdu, China. His research interests include networked control systems, multiagent systems, and robotics.

Prof. Yan is an Associate Editor of IEEE TRANSACTIONS ON NEURAL NETWORKS AND LEARNING SYSTEMS, *International Journal of Robotics and Automation*, and IEEE OPEN JOURNAL OF CIRCUITS AND SYSTEMS.

Hao Zhang received the B.Sc. degree in automatic control from the Wuhan University of Technology, Wuhan, China, in 2001, and the Ph.D. degree in control theory and control engineering from the Huazhong University of Science and Technology, Wuhan, in 2007.

From 2011 to 2013, she was a Postdoctoral Fellow with the City University of Hong Kong, Hong Kong. She is currently a Professor with the School of Electronics and Information Engineering, Tongji University, Shanghai, China. Her research interests include network-based control systems, multiagent systems, and UAVs.

Prof. Zhang is an Associate Editor of *IEEE Intelligent Transportation Systems Magazine*.

Meng Wang received the B.Eng. degree in automation from Northeastern University at Qinhuangdao, Qinhuangdao, China, in 2011, the M.Eng. degree in control science and engineering from the Harbin Institute of Technology, Harbin, China, in 2013, and the Ph.D. degree from the Department of Mechanical and Biomedical Engineering, City University of Hong Kong, Hong Kong, SAR, China, in 2018.

He is currently an Associate Professor with the School of Information Science and Engineering, East China University of Science and Technology, Shanghai, China. His research interests include robust control and filtering, fuzzy systems and control, and their engineering applications.

Lu Zeng received the B.S. degree in mechanical design, manufacturing, and automation from the East China University of Science and Technology, Shanghai, China, in 2008, and the M.S. degree in mechanical manufacturing and automation from Tongji University, Shanghai, in 2011. He is currently pursuing the Ph.D. degree with the School of Academy for Engineering and Technology, Fudan University, Shanghai.

His research interests include mobile robot and networked control systems.

Authorized licensed use limited to: CHONGQING UNIVERSITY. Downloaded on May 15,2023 at 10:16:35 UTC from IEEE Xplore. Restrictions apply.